



Master's thesis  
Astronomy

**Your Title Here**

Anni Järvenpää

October 25, 2017

Tutor: Professor Peter Johansson  
Dr. Till Sawala

Censors: prof. Smith  
doc. Smythe

UNIVERSITY OF HELSINKI  
DEPARTMENT OF PHYSICS

PL 64 (Gustaf Hällströmin katu 2a)  
00014 University of Helsinki





# Contents

<b>1</b>	<b>Introduction</b>	<b>1</b>
1.1	TL;DR version of prerequisite information . . . . .	1
1.2	History of Local Group Research . . . . .	1
1.3	Aim of This Thesis . . . . .	2
<b>2</b>	<b>Theoretical Background</b>	<b>3</b>
2.1	Expanding universe . . . . .	3
2.1.1	Discovery . . . . .	3
2.1.2	$\Lambda$ CDM Cosmology . . . . .	3
2.1.3	Hubble flow . . . . .	3
2.2	Local Group . . . . .	3
2.2.1	Spiral Galaxies . . . . .	4
2.2.2	Other Members of the Local Group . . . . .	6
2.2.3	Evolution . . . . .	8
2.2.4	Determining the Mass of the Local Group and Its Members . .	10
<b>3</b>	<b>general simulation thingies</b>	<b>11</b>
3.1	N-body simulations . . . . .	11
3.1.1	Hierarchical Tree Algorithm . . . . .	11
3.1.2	Numerical Integrators . . . . .	11
3.1.3	Halo Finding with Subfind . . . . .	11

3.2	Description of actual simulations used . . . . .	11
<b>4</b>	<b>Mathematical and statistical methods</b>	<b>12</b>
4.1	Statistical Background . . . . .	12
4.1.1	Hypothesis testing and p-values . . . . .	13
4.1.2	Distribution functions . . . . .	14
4.2	Linear Regression . . . . .	17
4.2.1	Simple linear regression . . . . .	18
4.2.2	Multiple linear regression . . . . .	20
4.3	Principal Component Analysis . . . . .	20
4.3.1	Extracting Principal Components . . . . .	21
4.3.2	Excluding Less Interesting Principal Components . . . . .	24
4.3.3	Principal Component Regression . . . . .	26
4.4	Error analysis . . . . .	26
4.5	Comparing two samples drawn from unknown distributions . . . . .	26
4.5.1	$\chi^2$ test . . . . .	27
4.5.2	Kolmogorov-Smirnov test . . . . .	30
4.5.3	Other tests based on EDFs . . . . .	34
4.6	Cluster Analysis . . . . .	35
<b>5</b>	<b>Findings from DMO Halo Catalogue Analysis</b>	<b>36</b>
5.1	Selection of Local Group analogues . . . . .	36
5.2	Hubble Flow Measurements . . . . .	36
5.3	Anisotropy of Hubble flow . . . . .	39
5.3.1	Clustering . . . . .	40
5.4	Statistical Estimate of the Local Group Mass . . . . .	41
<b>6</b>	<b>Conclusions</b>	<b>47</b>

Bibliography	48
A Principal Components	52

# 1. Introduction

## 1.1 TL;DR version of prerequisite information

1. galaxies form
  - Why?
  - When?
  - How?
  - Where?
2. galaxies form in groups
3. our local group is one of these
4. something about large scale distribution of galaxies

## 1.2 History of Local Group Research

LG objects visible with naked eye -> realization they are something outside our galaxy -> realization they are something very much like our galaxy

First determining distance was difficult, now mass is more interesting question

## 1.3 Aim of This Thesis

Whatever the main results end up being, presented in somewhat coherent manner and hopefully sugar-coated enough to sound Important and Exciting.



## 2. Theoretical Background

Think whether LG or LCDM first

### 2.1 Expanding universe

#### 2.1.1 Discovery

Make maths, add cosmological constant, make observations, remove cosmological constant

Enough cosmology here or in other sections to make other parts of thesis to make sense and to suffice as master's thesis = basic textbook cosmology and galaxy formation theory

#### 2.1.2 $\Lambda$ CDM Cosmology

#### 2.1.3 Hubble flow

What is, where seen, what means, how to measure, hotness/coldness

Plot: observations with fitted hubble flow

### 2.2 Local Group

vastaa kiusallisen

hyvin

introductionin

suunnitelmaa,

siirrä sinne

myöhemmin?

Our galaxy is one of the numerous galaxies that are a part of a galaxy group. According to Sparke and Gallagher (2007), around half of all galaxies are part of either a cluster or a group of galaxies where gravitational attraction of matter within the structure is strong enough to dominate over expansion of the universe. The two are distinguished by the mass of the association and number of objects in it: Sparke and Gallagher define systems with more than 50 luminous galaxies within a megaparsec from the center of the system as galaxy clusters whereas groups of galaxies have fewer members and often have masses less than  $10^{14} M_{\odot}$ .

tällä hetkellä tosi The Local Group with its three bright spirals and numerous smaller galaxies  
vähän siitä, miten scattered within roughly a megaparsec from the Milky Way and the Andromeda  
esim etäisyyksiä galaxy is a fairly typical galaxy group (Sparke and Gallagher, 2007). Due to prox-  
mitataan, pitäisikö imity of the members of the group, many objects can be resolved as individual stars  
olla enemmän? and even very faint objects can be detected, which makes the Local Group an excel-  
lent test laboratory to study interactions between galaxies. On the other hand, our  
location within the Milky Way makes estimating the brightness and other proper-  
ties of our own galaxy difficult and the extinction at the plane of the galaxy might  
obscure some faint members of the group (Sparke and Gallagher, 2007).

tämä ei varmaan The following sections shortly describe the structure, kinematics and evolution  
oikeasti johdattele of the Local Group with focus on the Milky Way and Andromeda galaxy pair, as  
sisältöön kovin these are the most prominent members and their coevolution is the most defining  
hyvin, mieti process in the Local Group. Their mutual dynamics also offer one way of estimat-  
sopivuus kun ing the mutual mass of the galaxy pair, which [jossain osassa esitellään, jossain  
varsinaiset arvioidaan vs muut menetelmät]. Many of the smaller members of the group are  
kappaleet ovat also satellites for either of the big galaxies and will eventually merge into their host.  
valmiita

### 2.2.1 Spiral Galaxies

jos jatkossakin  
sparkea, mainitse  
leipätekstissä ja  
skippaa yksittäiset  
viittaukset.  
Ajantasaisempi

Only three out of the more than 30 galaxies in the Local Group are spiral galaxies: the Andromeda Galaxy, its satellite M33 and our home galaxy, the Milky Way. These three galaxies dominate the Local Group in multiple ways. First of all, the three spirals are the three most massive galaxies in the Local Group (Sparke and Gallagher, 2007). The three galaxies also emit a total of 90 % of all visible light of the Local Group, Andromeda being the most luminous with its  $27 \times 10^9 L_{\odot}$  V-band luminosity, followed by the Milky Way with its  $15 \times 10^9 L_{\odot}$  and the M33 at  $5.5 \times 10^9 L_{\odot}$  (Sparke and Gallagher, 2007). Due to the Milky Way and the M33 being the most massive members of the Local Group, the center of the local group is often considered to lie between the Milky Way and the Andromeda galaxy (Sparke and Gallagher, 2007).

DM mainitaan vain  
ohimennen,  
enemmän?  
Kerrotko  
ollenkaan, että  
MW & M31  
matkalla kohti  
toisiaan?

The three spirals of the group are fairly typical spiral galaxies with a slightly warped thin disk of stars, gas and dust with a central bulge, surrounded by globular clusters and residing in a dark matter halo. However, there are some differences between the galaxies in addition to M33 being considerably less luminous than the other two. Whereas bulge and core of M33 are very small relative to the size of the galaxy compared to ones in the Milky Way and Andromeda galaxy, the latter differ in the contents of the core (Sparke and Gallagher, 2007). In the core of the Milky Way, gas and dust accreting into the central black hole power the radio source Sagittarius A\* while the core of the Andromeda galaxy contains very little interstellar matter and M33 has a very low mass black hole or none at all (Sparke and Gallagher, 2007).

The spiral patterns of the galaxies also differ and thus the galaxies belong to different classes in the Hubble sequence, Milky way being an Sbc galaxy, the Andromeda galaxy falling in class Sb and M33 in Sc (Sparke and Gallagher, 2007). The Andromeda galaxy has tightly wound spiral arms, which makes seeing the spiral pattern very difficult and star-formation is concentrated in a 'ring of fire' encircling

the center of the galaxy at about 10 kpc distance (Sparke and Gallagher, 2007). M33 on the other hand has more open spiral arms where clumps of newly formed stars are clearly visible (Sparke and Gallagher, 2007).

tynkä kappale      The mutual gravitational attraction of the system is strong enough to locally overcome the expansion of the universe and thus we observe the Andromeda Galaxy having a velocity of about 110 km/s towards the Milky Way (van der Marel et al., 2012). This is also what allows the Milky Way and Andromeda to maintain a system of smaller satellite galaxies around them.

massa tänne vai      TODO: mass estimate  
toisaalle?

### 2.2.2 Other Members of the Local Group

Despite spirals dominating the local group with their mass, most of the galaxies in the Local Group are either dwarf spheroidals or irregular galaxies (Sparke and Gallagher, 2007). In fact, out of the 35 non-spiral members the Local Group listed by Sparke and Gallagher (2007) only one is an elliptical galaxy, rest of the galaxies being either dwarf spheroidals or irregular galaxies. This elliptical is a small satellite of the Andromeda galaxy, visible near or on top of the disk of the Andromeda Galaxy in many optical images of the galaxy.

Current list of Local Group members might not be complete though as it is possible that some members of the Local Group have not yet been discovered due to the heavy absorption in the plane of the Milky Way.(Sparke and Gallagher, 2007). New ultra-faint galaxies are also still discovered, for example Leo III in 2015 (Kim et al., 2015) and some of the eight companions discovered by Bechtol et al. (2015).

Most of the other galaxies in the Local Group are satellite galaxies of either the Milky Way or the Andromeda galaxy: both of them have about a dozen of known satellites that orbit the primary (Sparke and Gallagher, 2007). In addition to these, Sparke and Gallagher (2007) list 14 'free fliers' that are within 1 Mpc of

the center of the Local Group but do not lie close to any large galaxies. The M33 is also speculated to possibly have its own satellites (Chapman et al., 2013; Martin et al., 2009).

For the Milky Way, two most prominent satellites are the Large and Small Magellanic Clouds, a pair of irregular galaxies that are also the most massive galaxies in the Local Group after the three spirals. The galaxies appear as irregular cloud-like structures near each other on the southern sky (Sparke and Gallagher, 2007). Despite the irregular shape of the galaxies, the Large Magellanic Cloud is often considered to be a Magellanic spiral (SBm) instead of an irregular galaxy as it has a bar and one short spiral arm but no other characteristics of a spiral galaxy (Sparke and Gallagher, 2007). Both galaxies are rich in hydrogen and star clusters with evidence of active star-formation history, but curiously the Large Magellanic Cloud has very few stellar clusters with ages from four to ten Gyr whereas Small Magellanic Cloud does not have a similar gap in its star-formation history (Sparke and Gallagher, 2007). The galaxies are also connected by a bridge of gas and young star clusters and

Both the irregular shapes and the curious star formation histories are likely results of interactions between galaxies. The Magellanic clouds are on orbits that bring them close to the Milky Way and them appearing near each other on the sky is not by chance: the galaxies are also on orbits around each other (Sparke and Gallagher, 2007). These interactions have created a bridge of gas and young stars connecting the Magellanic clouds and multiple large gas clouds share the orbit of the Large Magellanic Cloud on its way around the Milky Way, seen as a stream of gas stretching around the sky as a more than  $100^\circ$  arc (Sparke and Gallagher, 2007). This gas is likely to have been ripped from the Large Magellanic Cloud by the Small Magellanic Cloud when they passed near each other on their orbit (Sparke and Gallagher, 2007).

### 2.2.3 Evolution

The Local Group is a dynamic system where the interplay of its members have affected the system in many ways that we can now observe, as will the composition of the group further change in the future when the gravitational interactions continue to shape the system (Sparke and Gallagher, 2007). The origins of the Local Group, as origins of all structure in our visible universe, lie in density perturbations in the early Universe, denser regions collapsing first followed by gradually less and less dense ones (Sparke and Gallagher, 2007). Further, the perturbations occur on multiple scales: the Local Group as a whole is overdense, but it consists of smaller but even denser clumps separated with areas where matter is more sparse (Sparke and Gallagher, 2007).

lyhyt, soossi

The baryonic matter alone is not able to explain the structures we observe today: as discussed in section [TODO], structure formation requires substantially more mass than is observed with electromagnetic radiation. Thus the processes discussed in this section are dominated by the dark matter content of the Universe with the baryonic matter merely following the gravitational lead of the dark matter.

The collapse of these denser areas that would later form the Local Group started with the collapse of the oversende clumps that would simultaneously fall towards the center of the larger-scale overdense region (Sparke and Gallagher, 2007). This results in some of the most central clumps merging and forming a single galaxy which other clumps forming smaller satellites around it (Sparke and Gallagher, 2007). This all happens on multiple scales, as for example in the Local Group Milky Way and the Andromeda Galaxy fall towards each other while both of them have their satellite galaxies, some of which are speculated to have their own satellite systems as mentioned in section 2.2.2.

lyhyt

These clumps of matter are irregularly shaped, which results in gravitational interactions between the clumps also applying torque to the matter and thus setting

the matter in rotation (Sparke and Gallagher, 2007). The infall of the matter due to gravity and collisions then further increases the rotational velocity as the angular momentum is approximately conserved in the collisions (Sparke and Gallagher, 2007).

One way of gaining insight into the evolution of matter in protogalaxies that would later form the galaxies in our Local Group is to observe the Milky Way, where observers can resolve many structures in greater precision than in any other place in the Universe. For example the metal-poor globular clusters encircling the Milky Way tend to each consist of stars with similar composition, which suggests that the globulars were born of small homogenous clouds of gas early in time, enriched by just a few supernova explosions (Sparke and Gallagher, 2007). The collapse of the gas into a cluster of stars may have begun either after a perturbation of some sort, such as a collision with another cloud, or the cloud just exceeds the Jeans mass (Sparke and Gallagher, 2007).

Many of the globulars are also on elongated orbits around the center of the Milky Way, which further suggests that they formed at an early time: as dissipates its kinetic energy in interactions much more efficiently than stars that almost never actually collide (Sparke and Gallagher, 2007). Thus the later a system has transformed from gaseous to mainly stellar, the more ordered rotation we observe. This can be seen both in the disks and haloes of spiral galaxies: the rotation in the thin disk, containing the youngest stars, is very ordered and the stars are on closely aligned nearly circular orbits, whereas thick disk that contains slightly older stars also has more scatter in their orbits, and the old stars of metal-poor halo have elongated orbits in random orientations (Sparke and Gallagher, 2007).

käytännössä kaikki  
käyttävät muotoa  
 $\text{km s}^{-1}$ , olisiko  
parempi?

The angular momentum of the stars also gives valuable information about the extent of the cloud of gas from which the stars and thus the galaxy have formed. According to Sparke and Gallagher (2007), simulations suggest that on average

particles in a protogalaxy attain about 5% of the velocity of a circular orbit at the radius of the particle. Now if the rotation curve and thus the potential of the modern-day galaxy is known, one can estimate the original extent of the gas cloud from the change of the angular momentum as the particle moves inward in the potential field (Sparke and Gallagher, 2007). Using a flat rotation curve with rotation velocity of 200 km/s, Sparke and Gallagher (2007) estimates that the gas has been accreted from around 100 kpc radius, an area much larger than the current about 15 kpc extent of the stellar disk.

M32 ehkä galaksin ydin

#### 2.2.4 Determining the Mass of the Local Group and Its Members



## **3. general simulation thingies**

Data used here from EAGLE which uses modified GADGET-2 which is a tree-code that uses leapfrog

### **3.1 N-body simulations**

#### **3.1.1 Hierarchical Tree Algorithm**

#### **3.1.2 Numerical Integrators**

#### **3.1.3 Halo Finding with Subfind**

### **3.2 Description of actual simulations used**

Volume, number of particles, compare to other simulations, where better and where maybe worse

Resimulation of interesting regions

Simulation has same parameters as EAGLE 800 Mpc volume used schaye 2015 paper DM-only parts: Volker-Springer Gadget and Gadget 2 papers 1999 and 2005 or something, gravity part is more interesting than SPH Zooms can use multiple meshes, only one is used here gravitational softening

## 4. Mathematical and statistical methods

täällä tarvittavat esitiedot ja önnönnöö, listaa mm. mitä aiot kertoa kunhan tiedät itsekään

### 4.1 Statistical Background

vähän parempi Precision of the used equipment limits accuracy of all data gathered from  
tässä kuin physical experiments, simulations or observations. Therefore the results are affected  
aiemman otsikon by the measurement process and the results have to be presented as estimates with  
alla some error, magnitude of which is affected by both number of data points and  
accuracy of the measurement equipment (Bohm and Zech, 2010).

Estimating errors for measured quantities offers a way to test hypotheses and compare different experiments (Bohm and Zech, 2010). This is done using different statistical methods, of which the main methods relevant for this thesis are covered here. The methods are shortly introduced in the following sections together with basic statistical concepts that are necessary to understand the methods.

### 4.1.1 Hypothesis testing and p-values

A common situation in scientific research is that one has to compare a sample of data points to either a model or another sample in order to derive a conclusion from the dataset. In statistics, this is known as hypothesis testing. For example, this can mean testing hypotheses such as "these two variables are not correlated" or "this sample is from a population with a mean of 1.0" (J. V. Wall, 2003). Next paragraphs shortly introduce the basic concept of hypothesis testing and methods that can be used to test the hypothesis "these two samples are drawn from the same distribution" following the approach of (Bohm and Zech, 2010) and (J. V. Wall, 2003).

The process of hypothesis testing as described by begins with forming of a null hypothesis  $H_0$  that is formatted such that the aim for the next steps is to either reject it or deduce that it cannot be rejected with a chosen significance level. Negation of the null hypothesis is often called research hypothesis or alternative hypothesis and denoted as  $H_1$ . For example, this can lead to  $H_0$  "this dataset is sampled from a normal distribution" and  $H_1$  "this dataset is not sampled from a normal distribution". Choosing the hypothesis in this manner is done because often the research hypothesis is difficult to define otherwise.

After setting the hypothesis one must choose an appropriate test statistic. Ideally this is chosen such that the difference between cases  $H_0$  and  $H_1$  is as large as possible. Then one must choose the significance level  $\alpha$  which corresponds to the probability of rejecting  $H_0$  in the case where  $H_0$  actually is true. This fixes the critical region i.e. the values of test statistic that lead to the rejection of the  $H_0$ .

This kind of probability based decision making is always prone to error. It is easy to see that  $\alpha$  corresponds to the chance of  $H_0$  being rejected when it is true. This is known as error of the first kind. However, this is not the only kind of error possible. It might also occur that  $H_0$  is false but it does not get rejected, which is known as error of the second kind.

kerro mikä  $\alpha$  ja  $N$   
käytössä  
myöhemmin  
kunhan tiedät

There is no one optimal way of choosing  $\alpha$ , but instead one should try to find a balance between false rejections of null hypothesis and not being able to reject null hypothesis based on the dataset even if in reality it might not be true. When sample size (often denoted  $N$ ) is large, smaller values of  $\alpha$  can often be used as decisions get more accurate when  $N$  grows. For example tässä työssä  $\alpha$  oli jokin ja  $N$  jotain muuta.

It is crucial not to look at the test results before choosing  $\alpha$  in order to avoid intentional or unintentional fiddling with the data or changing the criterion of acceptance or rejectance to give desired results. Only after these steps should the test statistic be calculated. If the test statistic falls within the critical region,  $H_0$  should be rejected and otherwise stated that  $H_0$  cannot be rejected at this significance level. The critical values for different test statistics are widely found in statistical textbooks and collections of statistical tables or they can be calculated using statistical or scientific libraries available for many programming languages.

Despite statistical tests having a binary outcome " $H_0$  rejected" or " $H_0$  not rejected", a continuous output is often desired. This is what p-values are used for. The name p-value hints towards probability, but despite it's name p-value is not equal to the probability that the null hypothesis is true. These p-values are functions of a test statistic and the p-value for a certain value  $t_{obs}$  of a test statistic gives the probability that under the condition that  $H_0$  is true, the value of a test statistics for a randomly drawn sample is at least as extreme as  $t_{obs}$ . Therefore if p-value is smaller than  $\alpha$ ,  $H_0$  is to be rejected.

### 4.1.2 Distribution functions

ei hyvä, harkitse  
esim  
<http://puppulause-generaattori.fi/?ava-insana=jakauma-funktio>

Some statistical tests such as the Kolmogorov-Smirnov test and the Anderson-Darling test make use of distribution functions such as cumulative density function (CDF) and empirical distribution function (EDF) in determining the distribution

from which a sample is drawn.

To understand CDF and EDF, one must first be familiar with probability density function (PDF). As the name suggests, PDF is a function the value of which at some point  $x$  represents the likelihood that the value of the random variable would equal  $x$ . This is often denoted  $f(x)$ . Naturally for continuous functions the probability of drawing any single value from the distribution is zero, so these values should be interpreted as depicting relative likelihoods of different values. For example if  $f(a) = 0.3$  and  $f(b) = 0.6$  we can say that drawing value  $b$  is twice as likely as drawing value  $a$ . (Heino et al., 2012)

Another way to use the PDF is to integrate it over semi-closed interval from negative infinity to some value  $a$  to obtain the CDF, often denoted with  $F(x)$ :

$$F(x) = \int_{-\infty}^x f(x') dx'. \quad (4.1)$$

This gives the probability of a random value drawn from the distribution having value that is smaller than  $x$ . Relation between the PDF and the CDF is illustrated in figure 4.1, where PDFs and CDFs are shown for three different distributions. It is easy to see the integral relation between PDF and CDF and how wider distributions have wider CDFs. (Heino et al., 2012)

Both the PDF and the CDF apply to whole population or the set of all possible outcomes of a measurement. In reality the sample is almost always smaller than this. Therefore one cannot measure the actual CDF. Nevertheless, it is possible to calculate a similar measure of how big a fraction of measurements falls under a given value. This empirical counterpart of the CDF is known as empirical distribution function (EDF), often denoted  $\hat{F}(x)$ , and for a dataset  $X_1, X_2, \dots, X_n$  containing  $n$  samples it is defined to be

$$\hat{F}(x) = \frac{1}{n} \sum_{i=1}^n I[X_i \leq x] \quad (4.2)$$

where  $I$  is the indicator function, value of which is 1 if the condition in brackets is

PDF määritelmä  
vaikea ymmärtää

esittelet nyt nolosti  
EDF:n nimeltä  
kahdesti, mieti  
ratkaisu

lisää johonkin  
selitys  
normaalijakauman  
parametreille

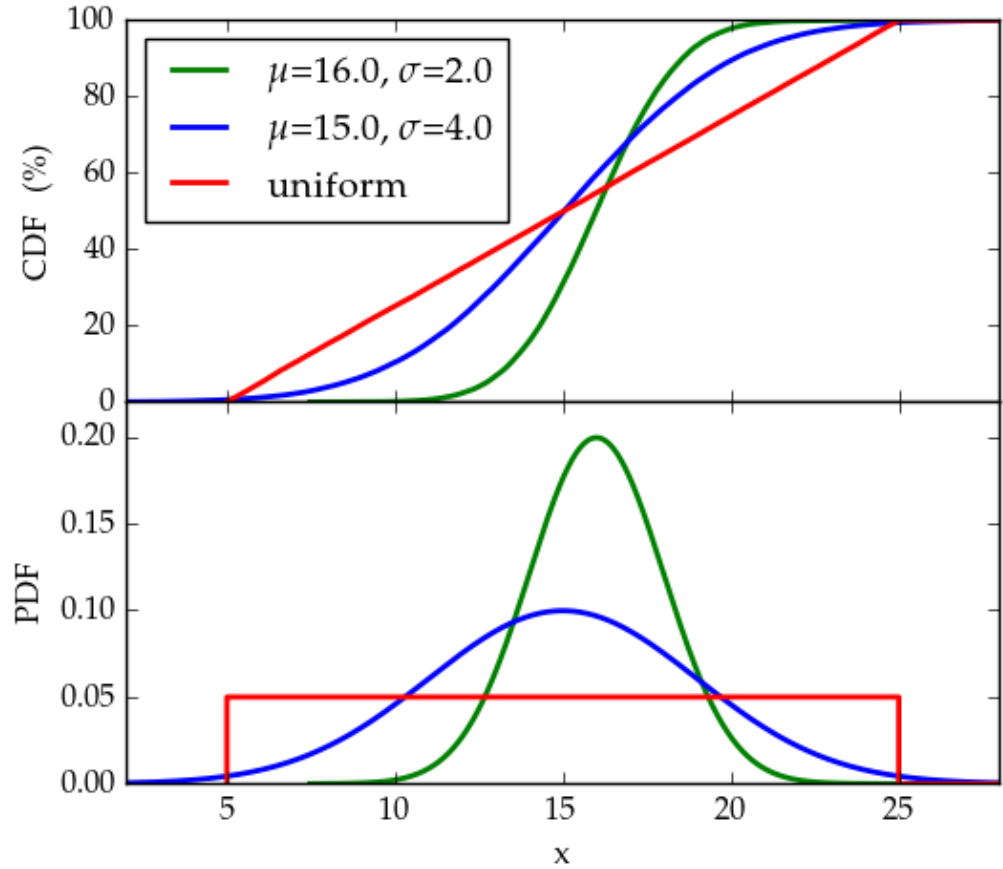


**Figure 4.1:** Cumulative distribution function (top panel) for three random samples (PDFs shown in the bottom panel) drawn from different distributions, two of which are normal and one is uniform. Parameters  $\mu$  and  $\sigma$  of the normal distribution describe the mean and the spread of the distribution respectively, large values of  $\sigma$  resulting in wide distribution.

true, otherwise 0. (Feigelson and Babu, 2012)

harkitse laittavasi  
jämpti arvo N:lle  
kun muut osat  
valmiita

Due to the EDF being a result of random sampling, it may deviate from the underlying CDF considerably as can be seen by comparing CDFs in figure 4.1 and corresponding EDFs in figure 4.2. This example is somewhat exaggerated with its  $N=35$  as the actual dataset used in this thesis has  $N>100$ , but reducing the sample size makes seeing the effects of random sampling easier. The latter figure also has EDFs corresponding to two random samples drawn from the distribution of the

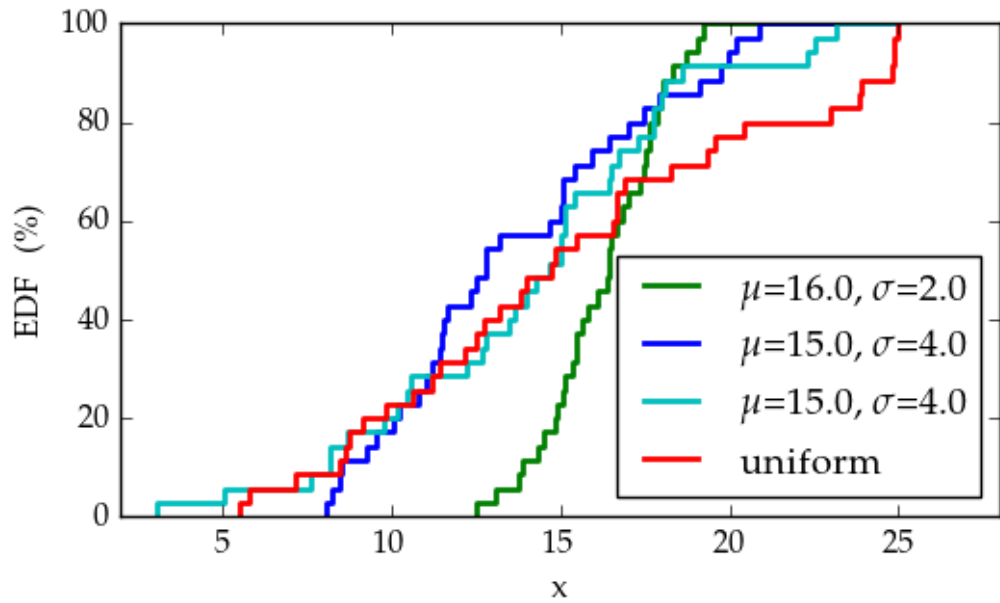


**Figure 4.2:** Empirical distribution function for four random samples ( $N=35$ ) drawn from the same distributions as in figure 4.1. Note that both the blue and the cyan data are drawn from the same distribution.

green curve in the first figure to further illustrate the differences that can arise from random sampling. This randomness also makes determining whether two samples are drawn from the same distribution difficult.

## 4.2 Linear Regression

Regression analysis is a set of statistical analysis processes that are used to estimate functional relationships between a response variable (denoted with  $y$ ) and one or more predictor variables (denoted with  $x$  in case of single predictor or  $x_1 \dots x_i$  if there are multiple predictor variables) (Feigelson and Babu, 2012). In this section, we will cover both simple regression where there is only one response variable and multiple linear regression where there are more than one response variables. The models also contain  $\varepsilon$  term that represents the scatter of measured points around

the fit. One of the models used is linear regression model, which can be used to fit any relationship where the response variable is a linear function of the model parameters (Montgomery, 2012). In addition to the widely known and used models where the relationship is a straight line, such as

$$y = \beta_0 x + \varepsilon \quad (4.3)$$

all models where relationship is linear in unknown parameters  $\beta_i$  are linear (Montgomery, 2012). Thus for example the following are linear models

$$y = \beta_0 x^2 + \varepsilon \quad (4.4)$$

$$y = \beta_0 e^x + \beta_1 \tan x + \varepsilon \quad (4.5)$$

$$y = \beta_0 + \beta_1 x_1 + \beta_2 x_2 + \varepsilon \quad (4.6)$$

On the other hand, all models where the relationship is not linear and therefore

$$y = x_0^\beta + \varepsilon \quad (4.7)$$

$$y = \beta_0 x + \cos(\beta_1 x) + \varepsilon \quad (4.8)$$

are nonlinear.

### 4.2.1 Simple linear regression

onko otsikko Simple linear regression is a model with a single predictor variable and a single  
järkevä kun response variable with a straight line relationship, i.e.

$$y = \beta_0 + \beta_1 x + \varepsilon \quad (4.9)$$

where parameter  $\beta_0$  represents the  $y$  axis intercept of the line and  $\beta_1$  is the slope of the line (Montgomery, 2012). The parameters can be estimated using method of least squares, where such values are found for the parameters that the sum of squared differences between the data points and the fitted line is minimized (Montgomery, 2012).



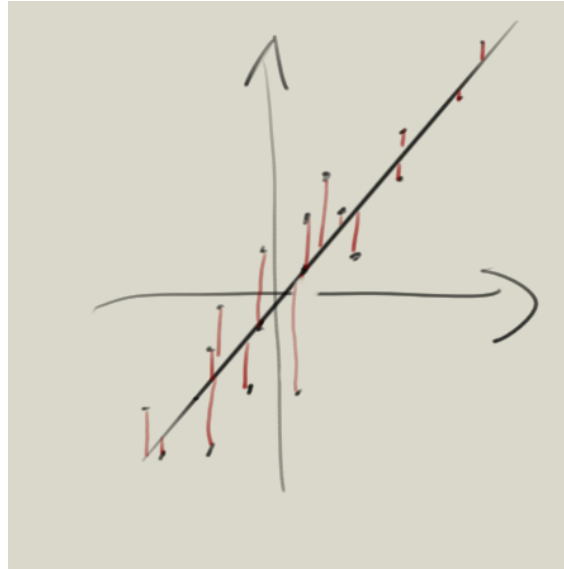


Figure 4.3

toisiko jotain lisää      The best-known method of minimizing the sum of squared error is the ordinary  
 jos olisi  $\beta_1$  ja  $\beta_2$  least-squares (OLS) estimator. The OLS method uses distances measured vertically  
 lausekkeet? as shown in figure 4.3 and thus the minimized sum is

$$\sum_{i=1}^n (y_i - \beta_0 - \beta_1 x_i)^2 \quad (4.10)$$

where  $x_1$  and  $y_i$  are single values of the measured quantities (Feigelson and Babu, 2012). This approach requires that the values of the predictor variable are known exactly without error and all uncertainty is in the values of the response variable (Feigelson and Babu, 2012). In those situations where this assumption is not valid, results acquired using OLS may be counterintuitive. This can be seen for example in figure 4.4 where OLS is used to calculate two linear fits: one where  $x$  is used and predictor variable and  $y$  as response variable and another where  $y$  is the predictor and  $x$  the response.

HF: OLS/TLS?      When dividing the variables to the independent variable with no error and a  
 Sido PCA:han response variable with possible measurement error is not a justifiable choice OLS  
 should not be used. One alternative for OLS is total least squares (TLS, also known as orthogonal least squares in some sources such as (Feigelson and Babu, 2012))

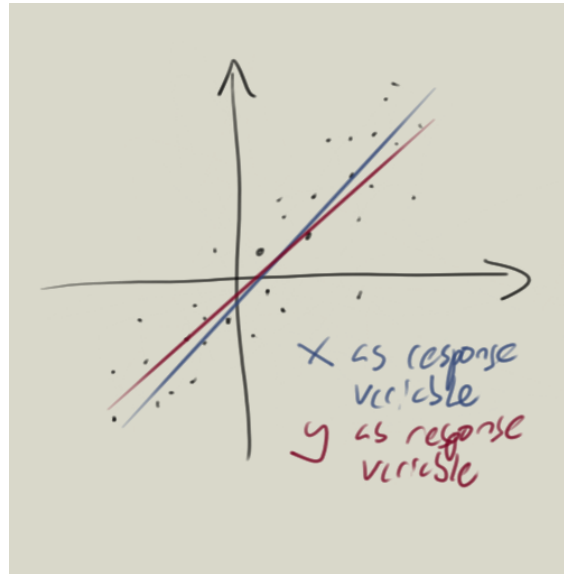


Figure 4.4

regression can be used instead of OLS (Markovsky and Huffel, 2007). The major difference between OLS and TLS is that instead of vertical distance, the minimized squared distance is measured between a point and its projection to the fitted line, thus providing minimum of the sum of the squared orthogonal distances from the line (Feigelson and Babu, 2012).

#### 4.2.2 Multiple linear regression

gradun sovellus: ongelman kuvailu, esim OLS:lle yleistys, jälleen liittyy PCA  
 onko PCR  
 relevantti?

### 4.3 Principal Component Analysis

orthogonal vs uncorrelated: Principal component analysis (PCA) is a statistical procedure first introduced by Pearson (1901) to aid physical, statistical and biological investigations where fitting a line or a plane to  $n$ -dimensional dataset is desired. When performing PCA, one transforms a data set to new set of uncorrelated variables i.e. ones represented by orthogonal basis vectors. These variables are called principal components (PCs)



Figure 4.5

(Jolliffe, 2002). This approach also solves the problem of sometimes arbitrary choice of division of the data to dependent and independent variables introduced in section 4.2.something Pearson (1901).

PCA can be used to both reduce and interpret data (Johnson, 2007). Often PCA alone does not produce the desired result, but instead PCs are used as a starting point for other analysis methods such as factor analysis or multiple regression (Johnson, 2007). These applications are introduced in the following subsections together with a short description of performing PCA and interpreting its results. In addition to these applications, PCA is also used in image compression, face recognition and other fields (Smith, 2002).

#### 4.3.1 Extracting Principal Components

In order to understand the process of obtaining principal components of a data set let us follow the procedure on a two-dimensional data set shown in the top panel of figure 4.6 with black dots. First step of finding the PCs is to locate the centroid of the dataset i.e. the mean of the data along every axis (Smith, 2002). This is marked

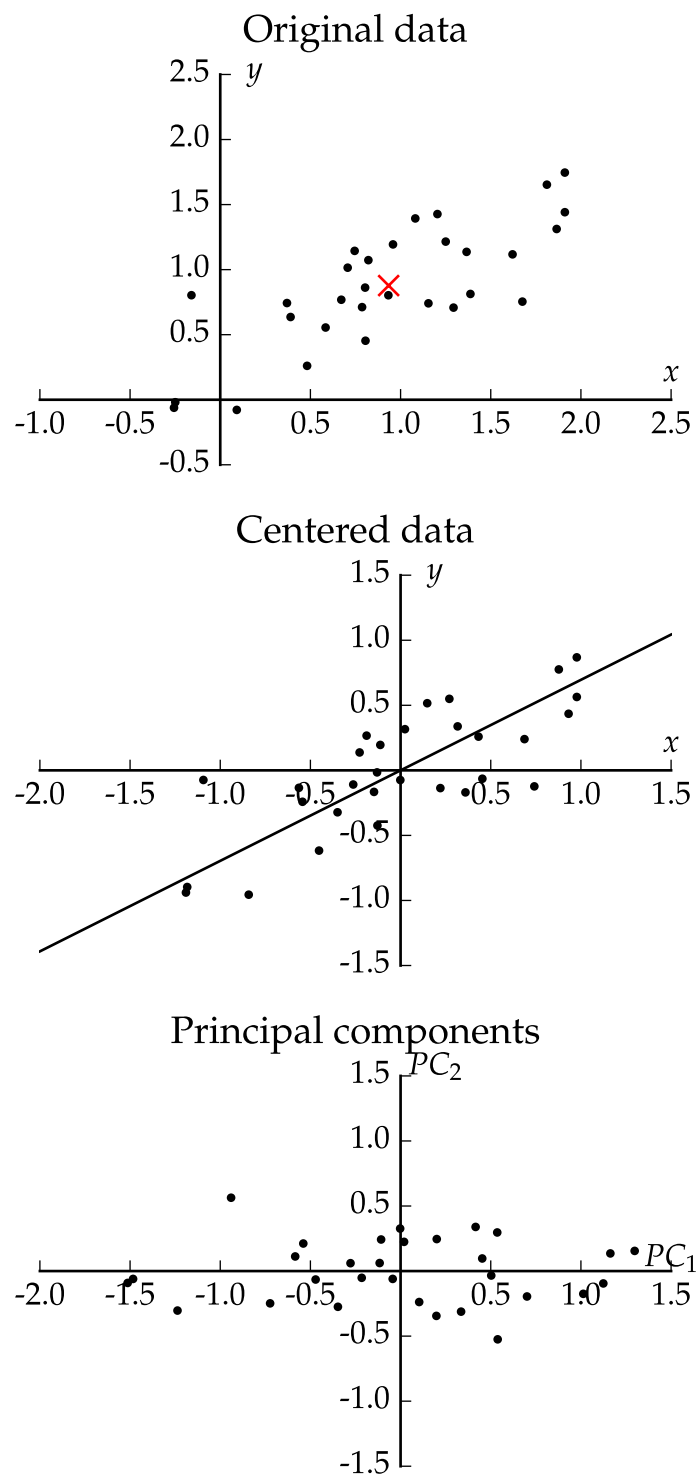


Figure 4.6: .

with a red x in the top panel of figure 4.6.

jos päädyt The best-fit line and therefore the PCs always pass through the centroid of the  
puhumaan system (Pearson, 1901), so subtracting the location of the centroid from the data  
eigenvektoreista tai is a natural next step, as this ensures that in the next step only the slope has to  
kovarianssimatrii- be optimized. This is done in the middle panel of the figure 4.6. If the variables  
seista, selitä ne have different units, each variable should be scaled to have equal standard devia-  
täällä tions (James et al., 2013) unless the linear algebra based approach with correlation  
matrices, as explained in e.g. (Jolliffe, 2002), is used.

If this scaling is not performed, the choice of units can arbitrarily skew the principal components. This is easy to see when considering for example a case where one has distances to galaxies in megaparsecs and their masses in units of  $10^{12} M_{\odot}$ , both of which might result in standard deviations being of the order of unity and PCA might thus yield principal components that are not dominated by neither variable alone. Now, say another astronomer has a similar data set, but distances are given in meters. In this case, most of the variation is in the distances, so distances will also dominate the PCs. If all variables are measured in the same units, scaling can be omitted in some cases (James et al., 2013).

Now the first PC can be located by finding the line that passes through the origin and has the maximum variance of the projected data points (Jolliffe, 2002), shown with a black line in the middle panel of figure 4.6 for our data set. PCs are always orthogonal and intersect at the origin, so in the two-dimensional example case the second and final PC is fully determined. The data set can now be represented using the PCs as is shown in the bottom panel of the figure 4.6.

Had the data set had more than two dimensions, the second PC would have been chosen such that it and the first PC are orthogonal and that variance along the new PC is again maximised (Jolliffe, 2002). This can be repeated for each dimension of the data set or, if dimensionality reduction is desired, only for a smaller number

of dimensions.

mieti mitä  
monospeissillä ja  
ole konsistentti

This level of understanding is often enough to successfully apply PCA to a problem, because PCA has ready-made implementations for many programming languages such as `prcomp` in R (James et al., 2013) and `sklearn.decomposition.PCA` in scikit-learn library (Pedregosa et al., 2011) for Python. If a more mathematical approach is desired, Smith (2002) explains PCA together with covariance matrices, eigenvectors and eigenvalues required to understand the process very clearly. Jolliffe (2002) also includes a very thorough description of PCA.

### 4.3.2 Excluding Less Interesting Principal Components

maininta  
bootstrappingista  
(loppuun?) ja siitä,  
että maistuu  
koneoppiminen?

Even though a data set has as many principal components as there are measured variables, one is often not interested in all of them as the last principal components might explain only a tiny fraction of the total variation in the data (James et al., 2013). Reducing the dimensionality of the problem also greatly eases visualizing and interpreting the data. Thus one might want to retain only first few of the PCs when PCA is used to for example compress, visualize or just interpret the data set at hand (James et al., 2013; Johnson, 2007). Unfortunately, many of the rules and methods used to determine the number of PCs to retain are largely without a formal basis or require assuming a certain distribution which is often not justifiable with the data (Jolliffe, 2002). With careful consideration these methods can nevertheless aid a researcher in making informed decisions and reasoned conclusions, so some rules are introduced in this section.

If the PCA is performed to aid visualizing the data set, retaining only the two first PCs can be a justified choice as two is the maximum number of dimensions that are easy to visualize on two-dimensional media such as paper and the two first PCs determine the best-fit plane for the data (Jolliffe, 2002). Of course the question whether the two PCs are sufficient to describe the data reasonably well still remains

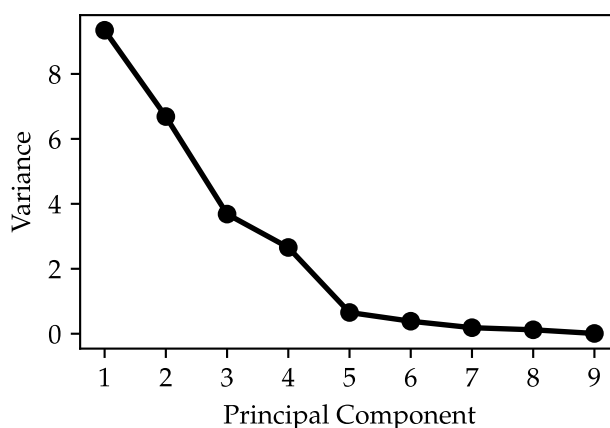


**Figure 4.7:** Example of a scree plot of randomly generated normally distributed data. In this case the plot has a clear elbow at fifth PC with the PCs 5-9 appearing roughly on a line. Thus the last five PCs could be a good number of PCs to be omitted if dimensionality reduction is desired.

unanswered in this case. Fortunately it can be addressed using some of the following methods used in general case of determining how many PCs to retain.

One widely used technique was introduced by Cattell (1966) to be used in factor analysis, but is also very much applicable to PCA (Jolliffe, 2002). This so called Cattell scree test involves plotting the variance of the data points along each PC versus the index of the PC. These plots tend to look similar to what is shown in figure 4.7, resembling a steep cliff with eroded material accumulated at the base, which is why these plots are known as scree plots and the nearly linear section of the plot is called the scree.

When the scree plot has two clearly different areas, the steep slope corresponding to the first PCs and a more gently sloping scree for the latter PCs, locating this elbow in the plot connecting the two areas will give the number of PCs that should be included (Jolliffe, 2002), which in case of figure 4.7 would yield five PCs. Some sources such as (Cattell, 1966) suggest that in some cases the PC corresponding to

the elbow should be discarded, which will result in one less PC.

Unfortunately, as Cattell also acknowledges in his paper, all cases are not as easy to analyze as the one in figure 4.7 and may prove difficult to discern for an inexperienced researcher. This problem might arise from for example noise in the linear part of the plot or scree line consisting of two separate linear segments with different slopes. The first case has no easy solution, but in the latter case Cattell suggests using the smaller number of PCs.

joku kiva lopetus  
tämän jälkeen?

Another straightforward method for choosing how many PCs to retain is to examine how much of the total variation in data is explained by first PCs and including components only up to a point where pre-defined percentage of the total variance is explained (Jolliffe, 2002). Whereas the previous method posed a challenge in determining which PC best matches the exclusion criteria, when using this approach the problem arises from choosing the threshold for including PCs. Jolliffe (2002) suggests that a value between 70 % and 90 % of the total variation is often a reasonable choice, but admits that the properties of the data set may justify values outside this range. Unfortunately, the suggested range is quite wide, so it may contain multiple PCs and therefore it is up to the researcher to determine the best number of PCs, while the criterion again acts as only an aid in the process.

### 4.3.3 Principal Component Regression

## 4.4 Error analysis

TODO: oispa  
parempi otsikko.  
mieti, onko tämä  
muutenkaan hyvä  
nyt kun on siirretty  
yksi otsikkotasoa  
ylöspäin

## 4.5 Comparing two samples drawn from unknown distributions



A common question in multiple fields of science is whether two or more samples are drawn from the same distribution. The most relevant methods that can be used to address this problem are introduced here following (Bohm and Zech, 2010) and (Feigelson and Babu, 2012) apart from introducing the  $\chi^2$  test which is mostly based on the approach of (Corder, 2014).

Questions related to comparing samples can emerge for example when comparing effectiveness of two procedures, determining if the instrument has changed over time or whether observed data is compatible with simulations. There are multiple two-sample tests that can address this kind of questions, e.g.  $\chi^2$ , Kolmogorov-Smirnov, Cramér-von Mises and Anderson-Darling tests.

In addition to comparing two samples, these tests can be used as one-sample tests to determine whether it is expected that the sample is from a particular distribution. However, some restrictions apply when using the one-sample variants. Some of these tests use categorical data, i.e. data where variables fall in pre-defined categories, and compares numbers of samples in different categories, whereas the others are applied to numerical data and compare empirical distribution functions (EDF) of the datasets.. Examples of such categories might be for example "galaxies that are active" or "data points between values 1.5 and 1.6".

#### 4.5.1 $\chi^2$ test

keksi paremmat      Astronomical data often involves classifying objects into categories such as  
esimerkit koko      "stars with exoplanets" and "stars without exoplanets" or the spectral classes of  
kappaleeseen,      stars (Feigelson and Babu, 2012). One tool for analyzing such categorical data is  
jotain relevanttia       $\chi^2$  test, which can be used both to determine whether a sample can be drawn from  
myöhempää      a certain distribution and to test whether two samples can originate from a single  
tutkimusta      distribution.  
ajatellen. katso  
kommentit      The method described here is sometimes referred to as Pearson's  $\chi^2$  test due  
paperista sen  
jälkeen, kaikkia ei  
täällä vielä

Stellar class	Number of observed planetary systems
A	6
F	38
G	39
K	134

**Table 4.1:** Example of categorical data.

to existence of other tests where  $\chi^2$  distribution is used. In some cases, such as with small  $2 \times 2$  contingency tables and when expected cell counts are small, other variants of  $\chi^2$  test should be used. For example the Yates's  $\chi^2$  test or the Fisher exact test work better in these cases than the  $\chi^2$  test.

For one-sample test, the  $\chi^2$  test uses the number of measurements in each bin together with a theoretical estimate calculated from the null hypothesis. For example one might have observed exoplanets and tabulated the number of planet-hosting stars of different spectral class as is shown in table 4.1 and now wants to test the observations against null hypothesis "Distribution of stellar classes for observed exoplanet-hosting stars is equal to that of main sequence stars in solar neighbourhood as given by Ledrew (2001)" using significance level  $\alpha = 0.01$ . The data is categorical, so now  $\chi^2$  test is a justified choice.

In this case the first step would be to calculate the expected observation counts for each bin according to the null hypothesis. Table 4.2 contains these expected counts ( $f_e$ ) together with the observations ( $f_o$ ). These observed and expected values are then used to calculate the  $\chi^2$  test statistic, defined as

$$\chi^2 = \sum_i \frac{(f_o - f_e)^2}{f_e}. \quad (4.11)$$

With the data given above this results in  $\chi^2 \approx 23.6$ . The data has four bins, so the degree of freedom is  $4 - 1 = 3$ . Next one can compare the calculated  $\chi^2$  value

Stellar class	Observations ( $f_o$ )	Theory ( $f_e$ )
A	6	6
F	38	28
G	39	71
K	134	112
total	217	217

**Table 4.2:** Data of table 4.1 together with expected values if null hypothesis was true.

to a tabulated critical value for our significance level  $\alpha = 0.01$ . These tabulated values can be widely found in statistics textbooks and books specifically dedicated to statistical tables.

In this case according to Corder (2014) the critical value is 11.34, which means that as  $23.6 > 11.34$  one can reject the null hypothesis and conclude that at 1% significance level the distribution of stellar classes for observed exoplanet-hosting stars is not equal to that of main sequence stars in solar neighbourhood. This of course can either be due to exoplanets being more numerous around some stellar classes than others or arise from some observational effect such as the observer observing more of the later type stars and thus arbitrarily skewing the distribution of the exoplanet finds.

The  $\chi^2$  test can also be used to test for independence of two or more samples. The data is again tabulated and now the  $\chi^2$  test statistic is calculated as

$$\chi^2 = \sum_i \sum_j \frac{(f_{oij} - f_{eij})^2}{f_{eij}} \quad (4.12)$$

where  $f_{oij}$  denotes the observed frequency in cell  $(i, j)$  and  $f_{eij}$  is the expected frequency for that cell. The expected frequency can be calculated using the following

formula

$$f_{eij} = \frac{R_i C_j}{N} \quad (4.13)$$

where  $R_i$  is the number of samples in row  $i$ ,  $C_j$  is the number of samples in column  $j$  and  $N$  is the total sample size.

According to Corder (2014), the degrees of freedom is  $(R-1)(C-1)$  where  $R$  is the number of rows and  $C$  is the number of columns in tabulated data. This is true in many if not most cases, but the way of collecting data can affect the degrees of freedom in both one-sample and multi-sample cases, as Press et al. (2007) explains. For example, if the one-sample model is not renormalized to fit the total number of observed events or, in two-sample case, the sample sizes differ, the degrees of freedom equal to number of bins  $N_b$  instead of  $N_b - 1$ .

Before performing the  $\chi^2$  test on a dataset, it is important to confirm that the data meets the assumptions for  $\chi^2$  test, given for example in (Bock et al., 2014) and (Heino et al., 2012). First of all, the data has to consist of counts i.e. not for example percentages or fractions. These counts should be independent of each other and there has to be enough of them, generally  $> 50$  is sufficient. Bins should also be chosen such that all bins have at least five counts according to the null hypothesis. If the last condition is not met, one can consider combining bins.

### 4.5.2 Kolmogorov-Smirnov test

For astronomers one of the most well-known statistical test is the Kolmogorov-Smirnov test, also known as the KS test. It is computationally inexpensive to calculate, easy to understand and does not require binning of data. It is also a nonparametric test i.e. the data does not have to be drawn from a particular distribution.

In the astrophysical context this is often important because astrophysical models usually do not fix a specific statistical distribution for observables and it is com-

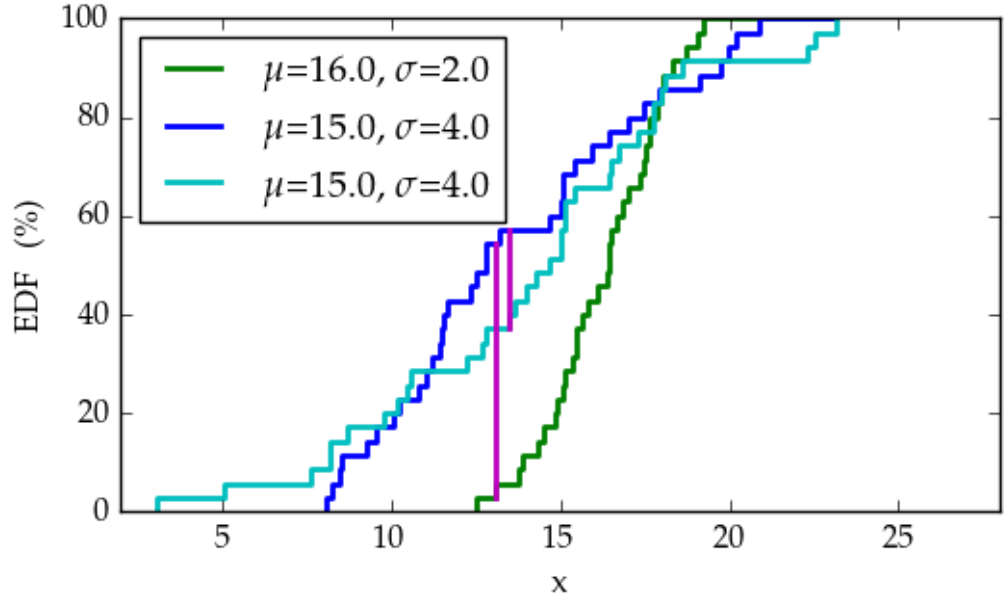


**Figure 4.8:** KS test parameter values (magenta vertical lines) shown graphically for three samples from figure 4.2.

mon to carry out calculations with logarithms of observables, after which the originally possibly normally distributed residuals will no longer follow a normal distribution. When using the KS test, the values on the x-axis can be freely reparametrized: for example using  $2x$  or  $\log x$  on x-axis will result in same value of the test statistic as using just  $x$  (Press et al., 2007).

The test can be used as either one-sample or two-sample test, both of which are very similar. For two-sample variate the test statistic for the KS test is calculated based on empirical distribution functions  $\hat{F}_1$  and  $\hat{F}_2$  derived from two samples and the test statistic

$$D = \sup_x |\hat{F}_1(x) - \hat{F}_2(x)| \quad (4.14)$$

uses the maximum vertical distance of the EDFs. This test statistic is then used to determine the p-value and thus decide whether the null hypothesis can be rejected. For one-sample variate the procedure is similar, but EDF  $\hat{F}_2$  is substituted with the CDF that corresponds to the null hypothesis.

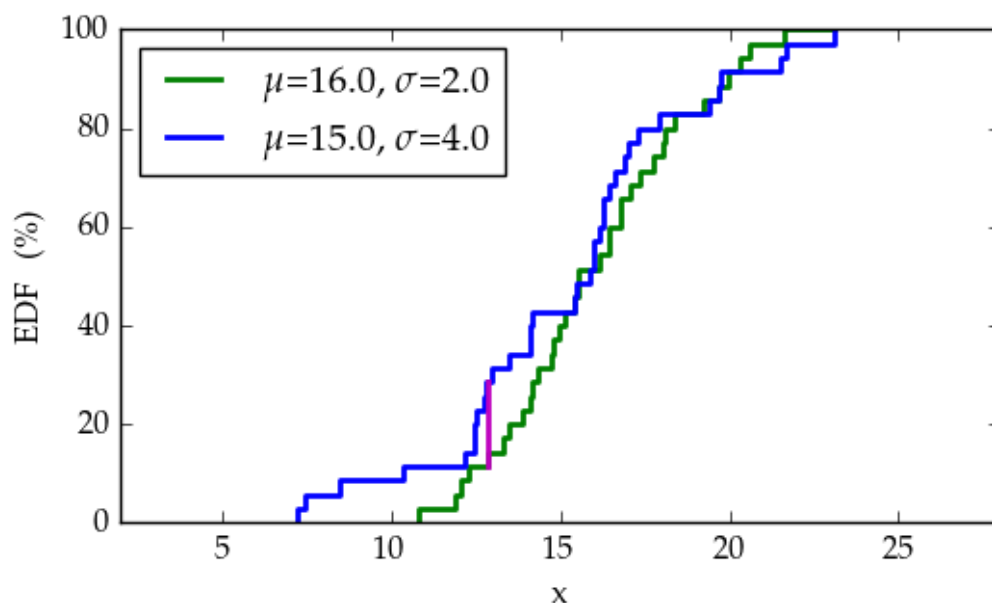


**Figure 4.9:** KS test ran on another pair of samples drawn from blue and green distributions in figure 4.1.

As an example, let us consider two pairs of samples from figure 4.2: green and blue (two samples drawn from different normal distributions) and blue and cyan (two samples drawn from same normal distribution). We can formulate the test and null hypotheses for both pairs as  $H_0$ ="the two samples are drawn from the same distribution" and  $H_1$ ="the two samples are not drawn from the same distribution" and choose a significance level of for example  $\alpha = 0.05$  or  $\alpha = 0.01$ .

mistä p-value  
saadaan, kerro taas  
aiemmin (tai  
täällä)

The test statistic is then calculated and for these samples we get  $D = 0.51$  for the green-blue pair and  $D = 0.20$  for the blue-cyan pair. Test statistics are illustrated in figure 4.8 where the test statistics  $D$  are shown as vertical magenta lines. According to Python function `scipy.stats.ks_2samp`, these values of  $D$  correspond to p-values  $9.9 \times 10^{-5}$  and 0.44 respectively, which means that the null hypothesis "green and blue samples are drawn from the same distribution" is rejected at both 0.05 and 0.01 significance levels but the null hypothesis "blue and cyan samples are drawn from the same distribution" cannot be rejected.

In this case the KS test produced result that matches the actual distributions from which the samples were drawn. Using a different random realization might have resulted in a different conclusion, for example one shown in figure 4.9 results in  $D = 0.17$  that corresponds to a p-value of 0.64 i.e. null hypothesis could not have been rejected using the  $\alpha$  specified earlier. In a similar manner there can be cases where two samples from one distribution are erroneously determined not to come from the same distribution if the samples differ from each other enough due to random effects.

The latter example case also illustrates one major shortcoming of the KS test: it is not very sensitive to small-scale differences near the tails of the distribution. For example in figure 4.9 the blue sample goes much further left, but because EDF is always zero at the lowest allowed value and one at the highest one the vertical distances near the tails are small and the test is most sensitive to differences near the median value of the distribution. On the other hand, the test performs quite well when the samples differ globally or have different means. (Feigelson and Babu, 2012)

The KS test is also subject to some limitations and it is important to be aware of them in order to avoid misusing it. First of all, the KS test is not distribution free if the model parameters, e.g. mean and standard deviation for normal distribution, are estimated from the dataset that is tested. Thus the tabulated critical values can be used only if model parameters are determined from some other source such as a simulation, theoretical model or another dataset.

Another severe limitation of KS test is that it is only applicable to one-dimensional data. If the dataset has two or more dimensions, there is no unique way of ordering the points to plot EDF and therefore if KS test is used, it is no longer distribution free. Some variants that can handle two or more dimensions have been invented, such as ones by Peacock (1983) and Fasano and Franceschini

"explain better"

(1987), but the authors do not provide formal proof of validity of these tests. Despite this, the authors claim that Monte Carlo simulations suggest that the methods work adequately well for most applications.

### 4.5.3 Other tests based on EDFs

ehkä vähän lyhyenpuoleisia kappaleita Unsatisfactory sensitivity of the KS test motivates the use of other more complex tests. Such tests are for example the Cramér-von Mises test (CvM) and Anderson-Darling (AD) test, both of which have their strengths. Similar to KS test, both of these can be used as one-sample or two-sample variants.

First of these tests integrates over the squared difference between the EDF of the sample and CDF from the model or two EDFs in case of two-sample test. The test statistic  $W^2$  for one-sample case can be expressed formally as

$$W^2 = \int_{-\infty}^{\infty} [\hat{F}_1(x) - F_0(x)]^2 dF_0(x) \quad (4.15)$$

For two-sample version, the theoretical CDF  $F_0$  has to be replaced with another empirical distribution function  $\hat{F}_2$ .

Due to integration, the CvM test is able to differentiate distributions based on both local and global differences, which causes it to often perform better than the KS test. Similar to the KS test, the CvM test also suffers from EDFs or an EDF and a CDF being equal at the ends of the data range, which again makes the test less sensitive to differences near the tails of the distribution.

In order to achieve constant sensitivity over the entire range of values, the statistic has to be weighted according to the proximity of the ends of the distribution. The AD test does this with its test statistic defined as

$$A^2 = N \int_{-\infty}^{\infty} \frac{[\hat{F}_1(x) - F_0(x)]^2}{F_0(x)[1 - F_0(x)]} dF_0(x) \quad (4.16)$$

where  $N$  is the number of data points in sample. This weighing makes the test more powerful than the KS and CvM tests in many cases. (Bohm and Zech, 2010;



Feigelson and Babu, 2012)

hnnngh Also other more specific tests exist, such as the Kuiper test which is well suited for cyclic measurements. The test should always be chosen to match the dataset such that it best differentiates between the null and research hypotheses.

## 4.6 Cluster Analysis

DBSCAN

# 5. Findings from DMO Halo Catalogue Analysis

## 5.1 Selection of Local Group analogues

criteria, how many found, what are like (some plots maybe? distributions of masses, separations, velocity components, number of subhaloes within some radius or correlations between two of those?). Some of this might be part of previous chapter too (relevant to resimulation)?

TODO: selitykset  
sille, miten osa on  
keskittynyt  
tiettyihin arvoihin  
sallitulla välillä ja  
osa jakautunut  
tasaisemmin.

Figure 5.1 shows how different features of the found LG analogues are distributed. TODO: selitykset  
sille, miten osa on keskittynyt tiettyihin arvoihin sallitulla välillä ja osa jakautunut tasaisemmin.

## 5.2 Hubble Flow Measurements

Mieti, pitäisikö  
kolme viimeistä  
esittää esim  
scatterplottina  
combined mass vs  
mass in more  
massive

HF, local  $H_0$ ,  $H_0$  within shells, zero-point, are previous consistent with what went into the simulation

Figure 5.2: two different simulations, MW-centered, huom obs nb how different they are: scatter, number of haloes, changes in scatter (bound structures)

Figure 5.3 shows haloes included and excluded in fitting, how is the process done

Figure 5.4 shows  $H_0$  at different radii. First bump is clear, latter ones not,

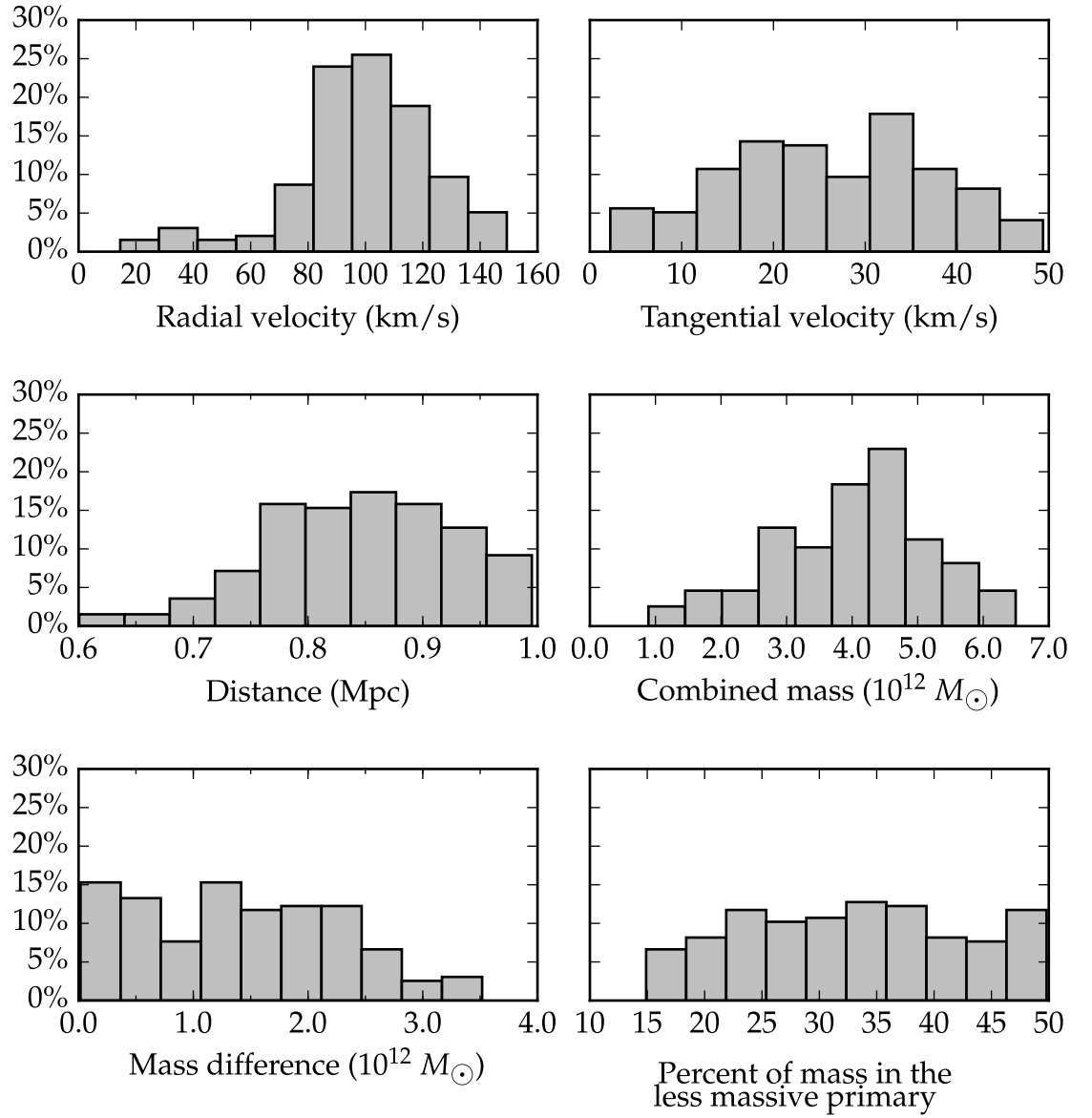


**Figure 5.1:** Distributions of LG analogue properties. TODO: selitä, mieti miten y-akselin label, binien rajat pitäisi pakottaa suurimpaan ja pienimpään sallittuun arvoon



**Figure 5.2:** Hubble Flows around Milky Way in two simulations.



**Figure 5.3:** HF slope: 86.9929348817

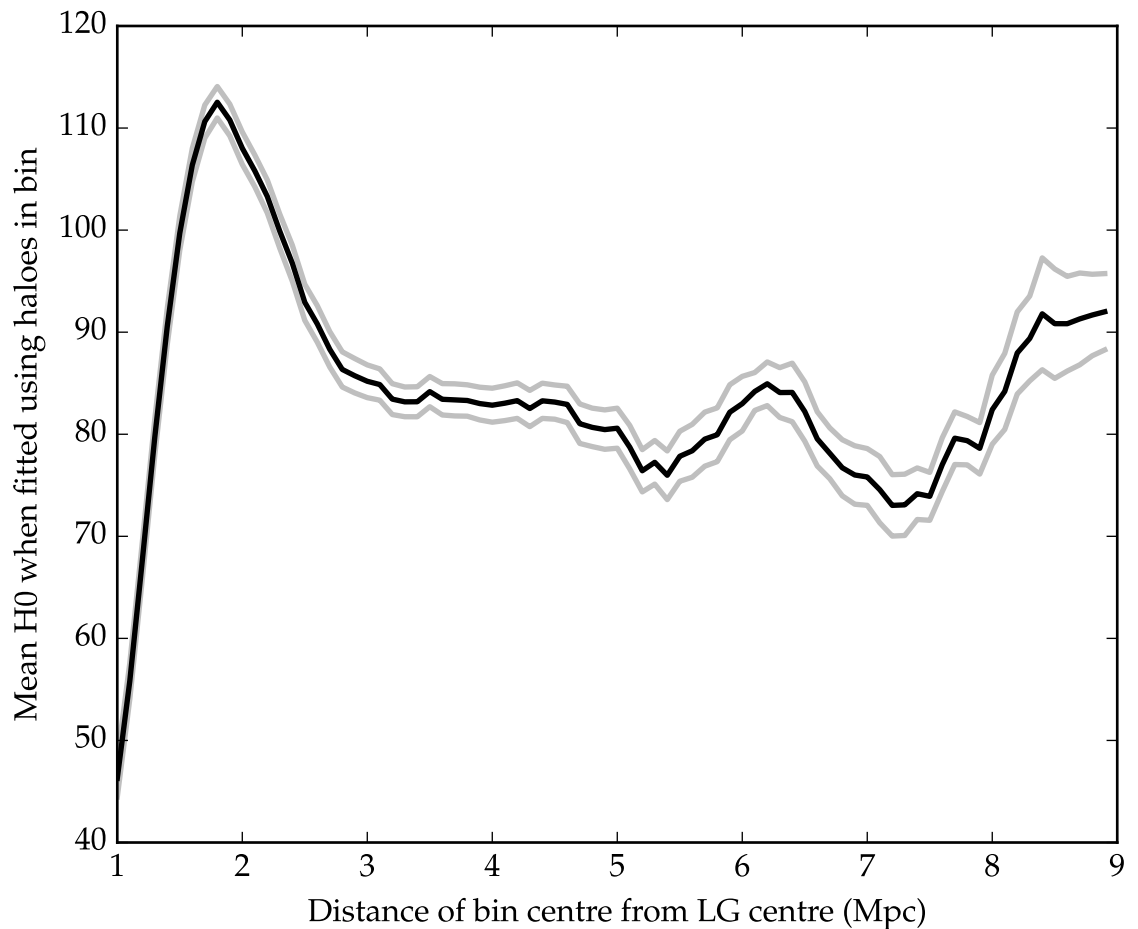


**Figure 5.4:** Mean  $H_0$  in different 2 Mpc bins, grey curves show standard error.

$H_0 > 67.7$  km/s, why. First ones have 350 samples, last ones only seven, remember to explain standard error. Figure 5.5 has bigger bins and shows zero points. Think whether both should use same plot type and which is better (line vs boxplot). If boxplot stays, change colours to all-black? At least explain what is what in plot.

X

### 5.3 Anisotropy of Hubble flow

isotropy + randomness or anisotropy? esittele konsepti. plots: see notebook last pages



**Figure 5.5:** HF zero point in different 4 Mpc bins. specify one outlier outside the plot

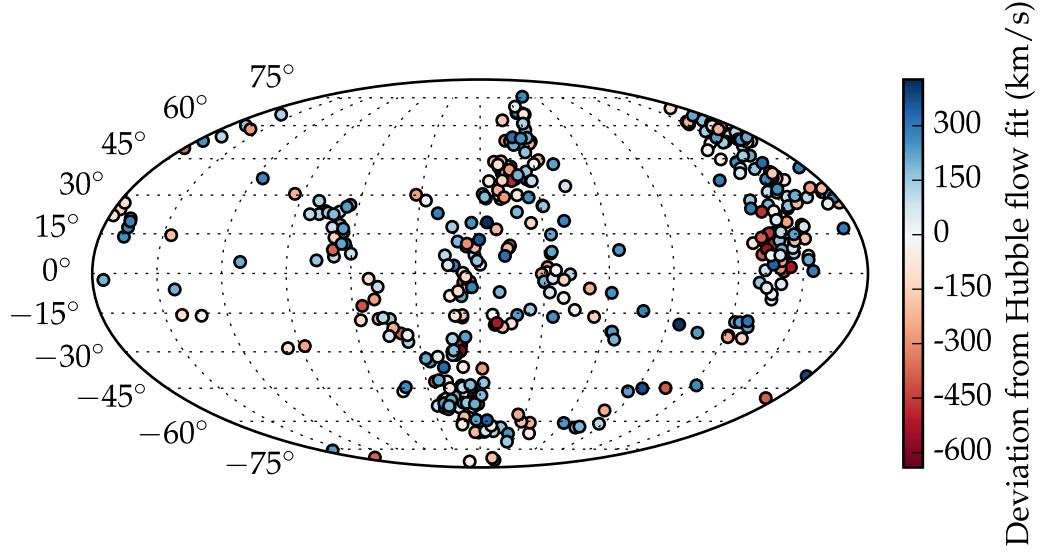
Simulaatio 97,  
esittele jo tässä  
näkyvät klöntit  
joissa paljon samaa  
väriä, näytä myös  
klusterointi ja  
vertaa löytöjä  
siihen

Figure 5.6 shows distribution of haloes around Milky Way analogue from one simulation with haloes closer than 1.5 Mpc away from center excluded to avoid cluttering the view with Andromeda counterpart and its satellites.

### 5.3.1 Clustering

Used DBSCAN introduced in [earlier chapter], angular distances of projections on sky as seen from MW.

Figure 5.8 shows the effect of varying minsamples and  $\epsilon$  on number of clusters found in each simulation ( $1.5 \text{ Mpc} < r < 5.0 \text{ Mpc}$  again). Regions where there are



**Figure 5.6:** Projections of haloes around the less massive LG primary with distances ranging from 1.5 Mpc to 5.0 Mpc.

ridiculously many clusters and ones where there are one or zero, relevant region in between, some areas have similar number of clusters but do the clusters look the same, see plots that don't exist yet

TODO: mieti  
laitatko samaan  
figureen, vertaile  
kuitenkin, selitä  
Ehkä vähän  
vasemmanpuolim-  
vähemmän tilaa  
mainen  
plottien välissä  
Massalysinä  
vaakasunnassa?  
Kaksi eri  
Keltaiset vähän  
kynnystä? Liian  
turhan samanlaisia.  
kapea ja  
epätasapainoinen,  
laita päällekkäin?

Figure 5.9 shows the change in mean diameter (supremum of angular distance between haloes) in cluster when  $\varepsilon$  and minsamples are varied. White areas where no clusters are found in any simulation.

Figures 5.10 and 5.11 show how the clustering results vary when clustering parameters are varied.

Figure 5.12 shows how derived values of slope and zero-point for the Hubble flow change when the Hubble flow fitting is carried out on partial data chosen based on the cluster membership of the haloes.

## 5.4 Statistical Estimate of the Local Group Mass

Analysis similar to Fattahi et al 2016 paper

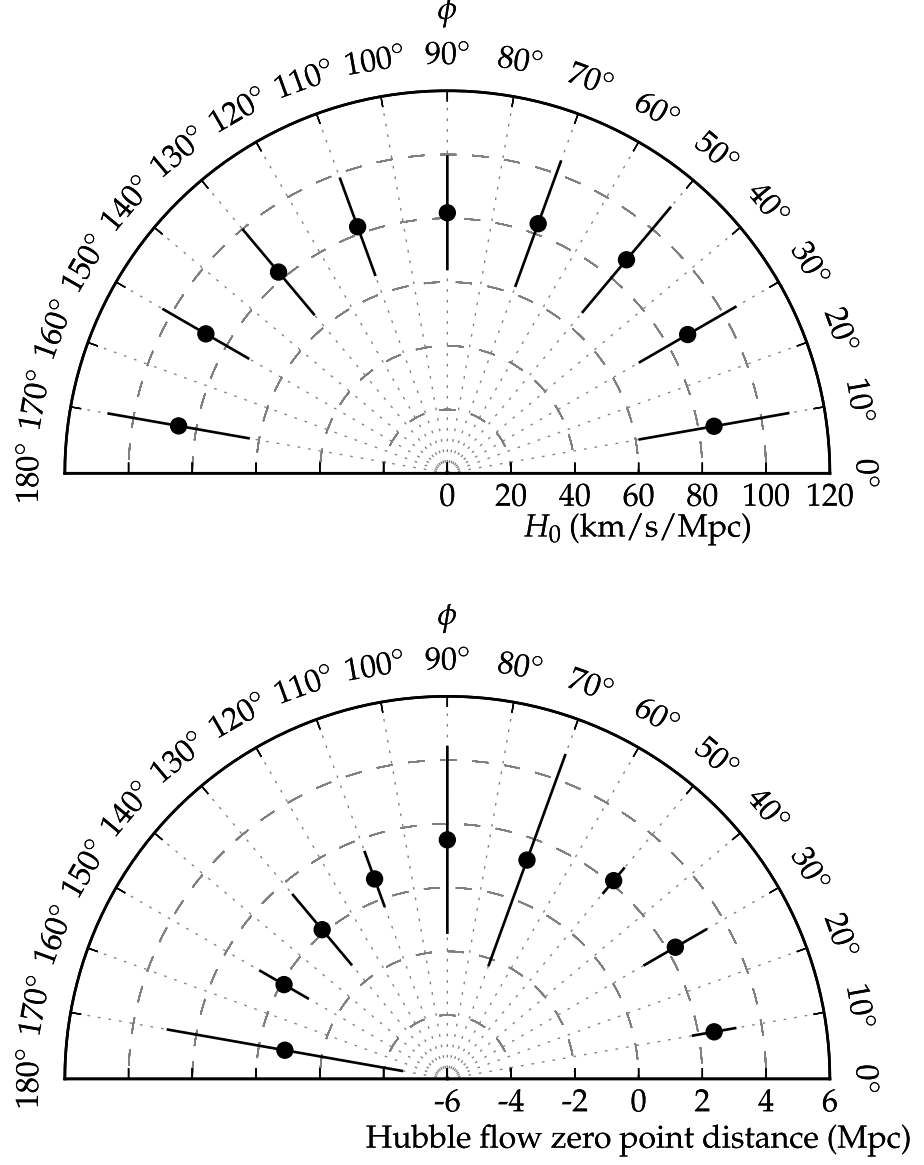


**Figure 5.7:** Mean Hubble flow slope and zero point as seen from Milky Way analogue in different  $20^\circ$  bins as measured from line connecting Milky Way and Andromeda analogues, direction  $0^\circ$  being towards Andromeda.



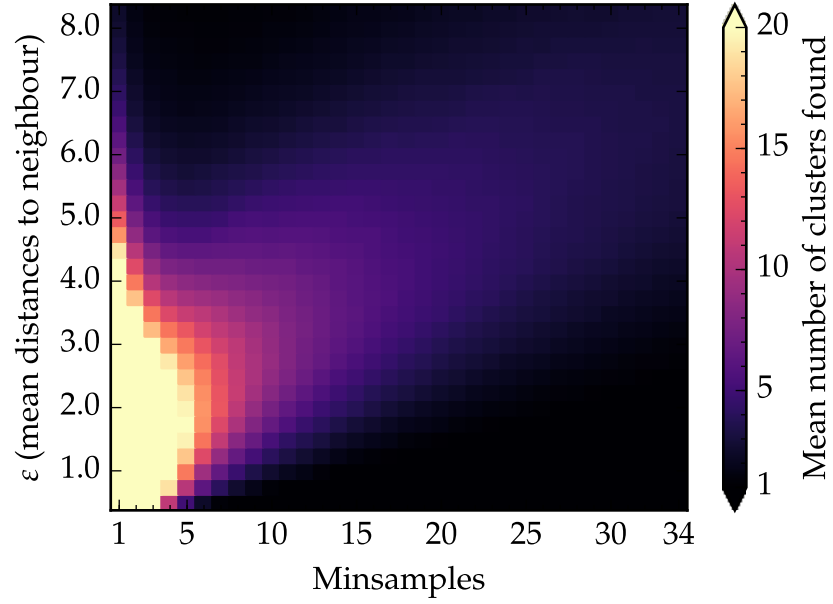


**Figure 5.8:** Mean number of clusters found for all simulations in dataset with different DBSCAN parameters. In all simulations  $\varepsilon$  is scaled using the mean distance between closest neighbours.



**Figure 5.9:** Mean diameter of clusters found for all simulations in dataset with different DBSCAN parameters. In all simulations  $\varepsilon$  is scaled using the mean distance between closest neighbours.



**Figure 5.10:** Results of DBSCAN clustering on same simulation output with different clustering parameters. TODO: mieti, kuuluuko tämäntyyppinen DBSCANin yleisiä ominaisuuksia esittelevä kuva enemmänkin teoriaosaan. Toisaalta selvästi dataspesifejä juttuja.

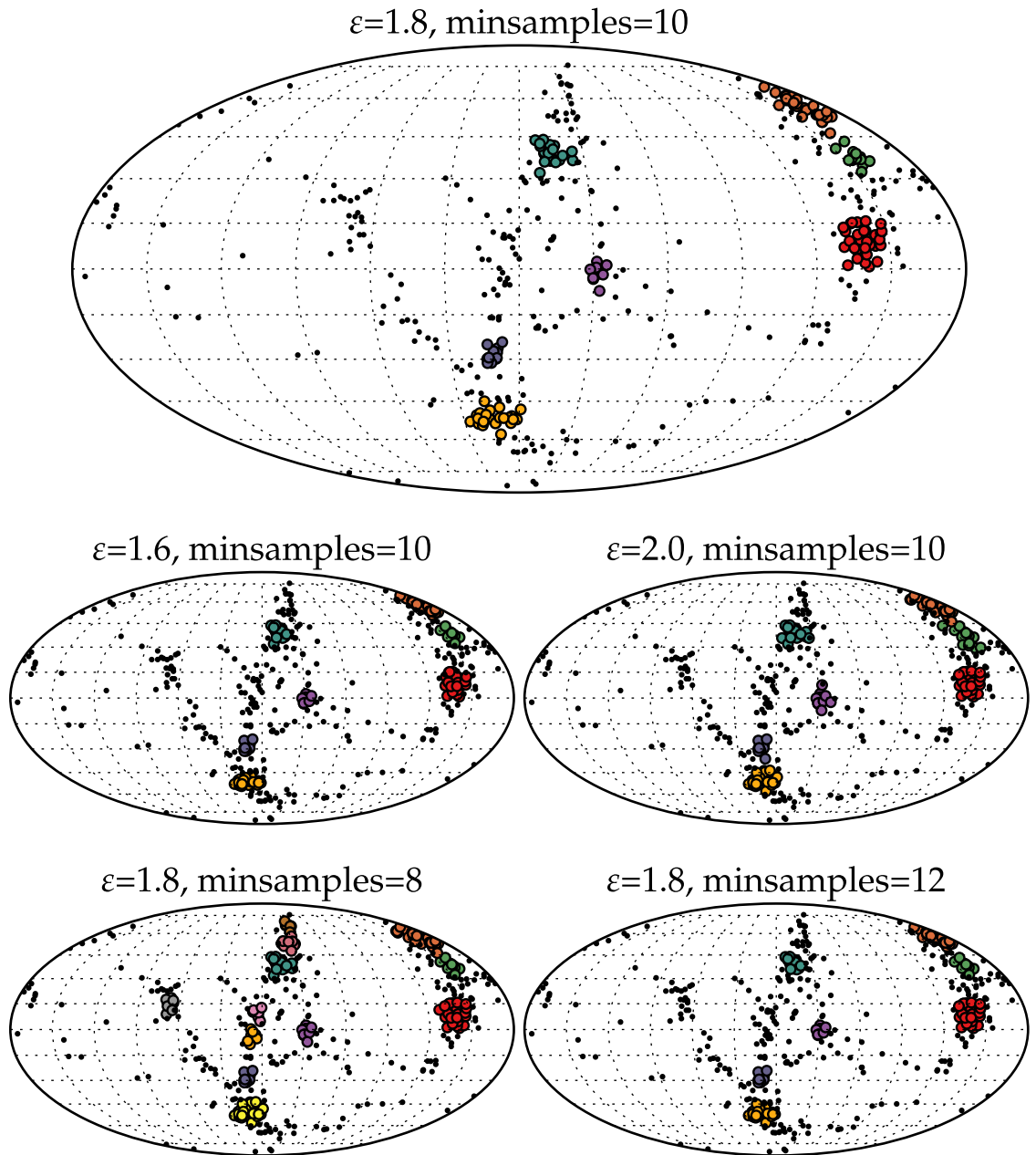


**Figure 5.11:** The effect of slightly varying the clustering parameters around the values  $\varepsilon=1.8$  and  $\text{minsamples}=10$  used when analyzing clustered data.

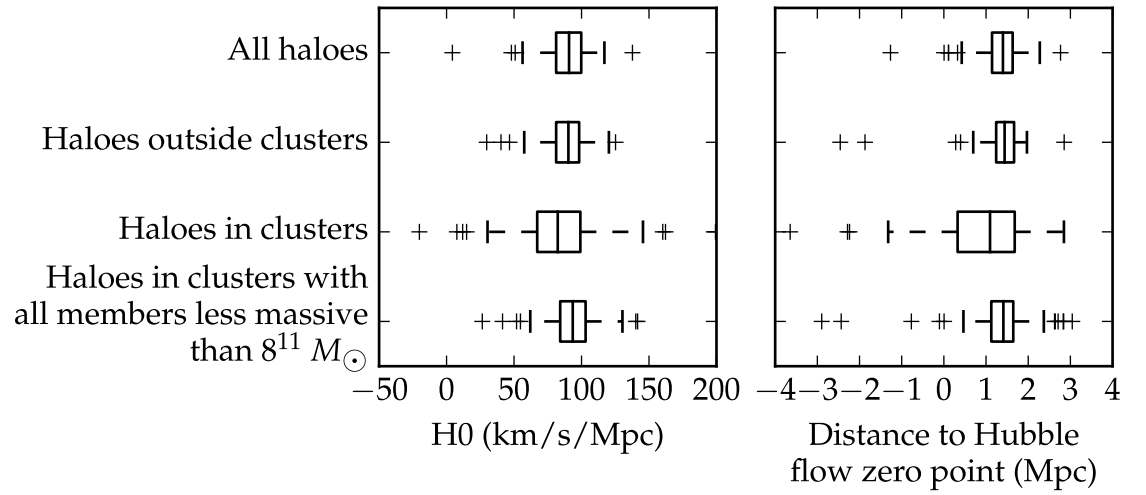


**Figure 5.12:** Hubble constant and distance to the point at which velocity due to the fitted Hubble flow is zero calculated from different samples. HUOM OBS NB erittele plotin ulkopuolelle jääneet kaukaiset outlierit

## 6. Conclusions

# Bibliography

- K. Bechtol, A. Drlica-Wagner, E. Balbinot, A. Pieres, J. D. Simon, B. Yanny, B. Santiago, R. H. Wechsler, et al. Eight new milky way companions discovered in first-year dark energy survey data. *The Astrophysical Journal*, 807(1):50, 2015. URL <http://stacks.iop.org/0004-637X/807/i=1/a=50>.
- D. Bock, P. Velleman, and R. De Veaux. *Stats: Modeling the World*. Pearson, third edition edition, 2014.
- G. Bohm and G. Zech. *Introduction to statistics and data analysis for physicists*. DESY, 2010. ISBN 9783935702416. URL [http://www-library.desy.de/preparch/books/vstatmp\\_engl.pdf](http://www-library.desy.de/preparch/books/vstatmp_engl.pdf).
- Raymond B Cattell. The scree test for the number of factors. *Multivariate behavioral research*, 1(2):245–276, 1966.
- S. C. Chapman, L. Widrow, M. L. M. Collins, J. Dubinski, R. A. Ibata, M. Rich, A. M. N. Ferguson, M. J. Irwin, G. F. Lewis, N. Martin, A. McConnachie, J. Peñarrubia, and N. Tanvir. Dynamics in the satellite system of triangulum: is and xxii a dwarf satellite of m33? *Monthly Notices of the Royal Astronomical Society*, 430(1):37–49, 2013. doi: 10.1093/mnras/sts392. URL <http://dx.doi.org/10.1093/mnras/sts392>.
- F. Combes, P. Boissé, A. Mazure, and A. Blanchard. *Galaxies and cosmology*.

- Astronomy and astrophysics library. Springer, Berlin ; New York, 2nd ed edition, 2002.
- Gregory W. Corder. *Nonparametric statistics : a step-by-step approach*. Wiley, Hoboken, New Jersey, second edition edition, 2014.
- G. Fasano and A. Franceschini. A multidimensional version of the Kolmogorov-Smirnov test. *Monthly Notices of the Royal Astronomical Society*, 225:155–170, March 1987. doi: 10.1093/mnras/225.1.155.
- Eric D. Feigelson and G. Jogesh Babu. *Modern Statistical Methods for Astronomy: With R Applications*. Cambridge University Press, 2012. doi: 10.1017/CBO9781139015653.
- R. Heino, K. Ruosteenoja, and J. Räisänen. *Havaintojen tilastollinen käsittely*. Department of Physics (University of Helsinki), 2012.
- C. R. Jenkins J. V. Wall. *Practical Statistics for Astronomers*. Cambridge Observing Handbooks for Research Astronomers. Cambridge University Press, illustrated edition edition, 2003. ISBN 9780521454162,0521454166.
- G. James, D. Witten, T. Hastie, and R Tibshirani. *An introduction to statistical learning : with applications in R*. Springer texts in statistics. Springer, New York, 2013.
- Richard Arnold Johnson. *Applied multivariate statistical analysis*. Pearson Prentice Hall, Upper Saddle River, 6th ed edition, 2007.
- I. T. Jolliffe. *Principal component analysis*. Springer series in statistics. Springer, New York, 2nd edition edition, 2002.
- Dongwon Kim, Helmut Jerjen, Dougal Mackey, Gary S. Da Costa, and Antonino P. Milone. A hero’s dark horse: Discovery of an ultra-faint milky way satellite

- in pegasus. *The Astrophysical Journal Letters*, 804(2):L44, 2015. URL <http://stacks.iop.org/2041-8205/804/i=2/a=L44>.
- G. Ledrew. The Real Starry Sky. *Journal of the Royal Astronomical Society of Canada*, 95:32, February 2001.
- Ivan Markovsky and Sabine Huffer. Overview of total least-squares methods. 87: 2283–2302, 10 2007.
- Nicolas F. Martin, Alan W. McConnachie, Mike Irwin, Lawrence M. Widrow, Annette M. N. Ferguson, Rodrigo A. Ibata, John Dubinski, Arif Babul, Scott Chapman, Mark Fardal, Geraint F. Lewis, Julio Navarro, and R. Michael Rich. Pandas’ cubs: Discovery of two new dwarf galaxies in the surroundings of the andromeda and triangulum galaxies. *The Astrophysical Journal*, 705(1):758, 2009. URL <http://stacks.iop.org/0004-637X/705/i=1/a=758>.
- Douglas C. Montgomery. *Introduction to linear regression analysis*. Wiley series in probability and statistics. John Wiley & Sons Ltd, Hoboken, New Jersey, fifth edition edition, 2012.
- J. A. Peacock. Two-dimensional goodness-of-fit testing in astronomy. *Monthly Notices of the Royal Astronomical Society*, 202:615–627, February 1983. doi: 10.1093/mnras/202.3.615.
- Karl Pearson. LIII. On lines and planes of closest fit to systems of points in space. *The London, Edinburgh, and Dublin Philosophical Magazine and Journal of Science*, 2(11):559–572, 1901.
- F. Pedregosa, G. Varoquaux, A. Gramfort, V. Michel, B. Thirion, O. Grisel, M. Blondel, P. Prettenhofer, R. Weiss, V. Dubourg, J. Vanderplas, A. Passos, D. Cournapeau, M. Brucher, M. Perrot, and E. Duchesnay. Scikit-learn: Machine learning in Python. *Journal of Machine Learning Research*, 12:2825–2830, 2011.



William H. Press, Saul A. Teukolsky, William T. Vetterling, and Brian P. Flannery, editors. *Numerical recipes: The art of scientific computing*. Cambridge University Press, New York, third edition edition, 2007.

Lindsay I Smith. A tutorial on principal components analysis. 2002.

Linda S. Sparke and John S. Gallagher. *Galaxies in the universe: an introduction*. Cambridge University Press, Cambridge, New York, 2nd ed edition, 2007.

Roeland P. van der Marel, Mark Fardal, Gurtina Besla, Rachael L. Beaton, Sangmo Tony Sohn, Jay Anderson, Tom Brown, and Puragra Guhathakurta. The m31 velocity vector. ii. radial orbit toward the milky way and implied local group mass. *The Astrophysical Journal*, 753(1):8, 2012. URL <http://stacks.iop.org/0004-637X/753/i=1/a=8>.

## A. Principal Components

PC	$H_0$	HF zero (clustered)	HF zero (not clustered)	$\sigma_{radvel}$ (clustered)	$\sigma_{radvel}$ (not clustered)	$v_{r,LG}$	$v_{t,LG}$	$r_{LG}$	
1	-0.386	-0.449	-0.324	-0.393	-0.211	-0.384	-0.211	0.097	0.013
2	0.147	0.221	0.248	-0.064	-0.599	-0.056	-0.599	-0.103	0.332
3	0.287	0.145	0.186	-0.531	0.258	-0.535	0.258	0.115	0.313
4	0.009	0.020	-0.152	0.151	-0.047	0.136	-0.047	0.934	0.221
5	-0.024	-0.171	-0.273	0.140	0.134	0.227	0.134	-0.270	0.840
6	0.015	-0.092	0.706	0.049	0.065	0.072	0.065	0.147	0.127
7	-0.848	0.156	0.323	-0.074	0.071	0.060	0.071	-0.001	0.128
8	-0.162	0.582	-0.206	0.456	0.024	-0.529	0.024	-0.018	0.061
9	0.041	-0.572	0.239	0.549	-0.008	-0.452	-0.008	-0.016	0.031
10	0.000	-0.000	0.000	-0.000	0.707	-0.000	-0.707	0.000	-0.000

**Table A.1:** component  $H_0$ s zeropoints inClusterZeros outClusterZeros allDispersions clusterDispersions unclusteredDispersions radialVelocities tangentialVelocities LGdistances